THE JOURNAL OF PHYSICAL CHEMISTRY C

Article

pubs.acs.org/JPCC

Hydrogen Adsorption on PdGa(110): A DFT Study

P. Bechthold, P. Jasen, E. González, and A. Juan*

†Departamento de Física and IFISUR (UNS-CONICET), Universidad Nacional del Sur, Avenida Alem 1253, 8000 Bahía Blanca, Buenos Aires, Argentina

ABSTRACT: H and Pd bonding is analyzed using density functional theory (DFT) calculations. Changes in the electronic structure of PdGa(110) surface upon the introduction of one or two hydrogen atoms are addressed. H locates only on Pd atop geometry and no interaction with Ga is detected. The Pd−Pd bond strength decreases as the new Pd−H bond is formed. The effect of H is limited to its first Pd neighbor. An analysis of orbital interaction reveals that Pd−H bonding mainly involves Pd 5s and H 1s orbitals with less participation of Pd 5p and 4d orbitals.

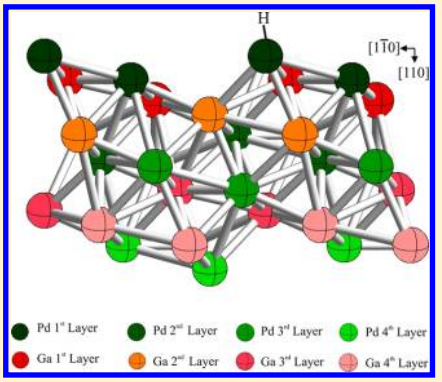

1. INTRODUCTION

Selective hydrogenation of acetylene ($C_2H_2 + H_2 \rightarrow C_2H_4$; $\Delta H = -172$ kJ/mol) is an important industrial process used to remove traces of acetylene in the ethylene feed for polyethylene production (>50 × 10^6 t/a). Acetylene has to be removed because it poisons the ethylene to polyethylene polymerization catalyst; therefore, through the use of a catalyst, the acetylene content in the ethylene feed has to be reduced to the lowest ppm range.[1−6] In order to decrease the cost for polyethylene production, a selective and stable hydrogenation catalyst is required for reducing the amount of acetylene in the feed without hydrogenating a large fraction of ethylene.[5]

Typical hydrogenation catalysts are made of palladium dispersed on metal oxides. Palladium metal exhibits high activity, though only limited selectivity. These kinds of catalysts frequently deactivate[4] under hydrogenation conditions by the formation of carbonaceous deposits resulting from the polycondensation of unsaturated compounds.[7]

Modification of these palladium catalysts by adding promoters or alloying with other metals has been shown to result in an increased selectivity and long-term stability in the hydrogenation of acetylene.[2] However, the catalytic performance of these modified Pd catalysts remains insufficient, and further improvements in selectivity may decrease the costs for polyethylene production. In addition to unsatisfactory selectivity, the long-term stability of palladium catalysts has to be improved.

Catalyst deactivation by carbonaceous deposits requires frequent exchange or regeneration of the catalyst in the hydrogenation reactor. Moreover, fresh or regenerated catalysts show high activity and local overheating of the reactor and, consequently, lead to increased ethylene consumption and selectivity loss.[6]

The limited selectivity of Pd catalysts in acetylene hydrogenation can be attributed to the presence of active-site ensembles on the catalyst surface.[2,6] Restricting the size of the active sites in a palladium-containing hydrogenation catalyst and thereby preventing the formation of ensembles of neighboring Pd atoms on the surface—so-called active-site isolation—may increase catalyst selectivity and long-term stability in acetylene hydrogenation. In addition to the presence of neighboring Pd atoms, the formation of palladium hydrides under hydrogenation reaction conditions substantially influences selectivity. Reducing the amount of the hydrogen incorporated into the catalyst decreases hydrogen supply for the hydrogenation reaction and increases the selectivity of acetylene hydrogenation to ethylene. It should also be mentioned that the modification of Pd-based catalysts by the presence of a second component in acetylene hydrogenation impacts at least two properties: the absorption of hydrogen and the formation of weakly adsorbed ethylene on the metal crystallite, or weakly π-bonded acetylene versus di-σ ethylene. Therefore, a depletion of (subsurface) hydrogen and/or a lower barrier of desorption of the carbonaceous intermediate—or acetylene adsorption—can modify the selectivity of palladium-based catalysts.[5]

The concept of using intermetallic compounds with covalent bonding rather than alloys is a suitable way to aim for long-term stable catalysts with preselected electronic and local structural properties.[7] The terms "intermetallic compound" and "alloy" are often confused in the literature. An "intermetallic compound", a chemical compound of two or more metallic elements that adopts at least a partly ordered crystal structure differing from those of the constituent metals, is a single-phase material and often holds a wide homogeneity range. On the other hand, an "alloy" is a mixture of metals, intermetallic

Received: March 17, 2012
Revised: July 5, 2012
Published: July 8, 2012

compounds, and/or non-metals, and thus it can contain more than one phase.[3]

Recently Armbrüster et al. reported that the presence of a Pd−Ga intermetallic compound is a highly active, selective, and stable catalyst for the semihydrogenation of acetylene in a large excess of ethylene.[8] The hydrogenation experiment detected no hydrogen uptake in PdGa, thus preventing a hydride formation that could lead to a reduction in catalytic activity.[9] Armbrüster et al. also described a strong covalent boundary between Pd and Ga atoms providing long-term stability for the catalysts under reaction conditions.[10]

The first synthetic route to single-phase nanoparticulate Pd_2Ga and PdGa was developed by Armbrüster et al.[11] Both systems show high selectivity and good long-time stability for the acetylene semihydrogenation. Catalytic properties can be transferred from a well-defined macroscopic model system to nanostructured materials prepared by coprecipitation of Pd, Ga, and Mg diluents.[12]

Active and selective Pd_2Ga intermetallic compounds supported on CNT were used in alkyne hydrogenation. Ordered structures form high barriers for subsurface chemistry and prevent large ensembles on the Pd surface.[13] Surface inspection of intermetallic PdGa $(\overline{1}11)$ reveals a smooth surface with a (1×1) unit cell where no segregation occurs. Co-adsorption properties indicate a bulk-truncated intermetallic compound with Pd−Ga partial covalent bonding.[14]

In our study, we selected gallium as part of the intermetallic compound, as it is known to be catalytically inactive in hydrogenation reactions and should not influence isolated Pd atoms in Pd−Ga intermetallic compounds. Hence, gallium acts as a spacer and forms the matrix for isolating Pd atoms. In the PdGa intermetallic compound, Pd atoms are separated from each other, and their atomic environment is fixed by the crystal structure, which should result in highly abundant single Pd sites on the surface. In turn, covalent interaction between Pd and Ga provides in situ stability for the crystal structure as well as polarization of Pd atoms in order to maximize the activation barrier for hydrogen atoms so as to enter into the bulk, thus preventing subsurface hydrogen formation and enhancing selectivity.[7]

2. SURFACE MODEL AND COMPUTATIONAL METHOD

The PdGa intermetallic compound presents a $P2_13$ structure with a lattice parameter of a_0 = 4.909 Å.[15−17] A refined crystal structure of (1:1) PdGa was recently reported.[19] This intermetallic compound has a simple cubic distortion (see Figure 1a), where each Pd is surrounded by seven Ga atoms (see Figure 1b). We selected the (110) crystallographic plane because it is the cleavage plane and could be exposed as a catalytic surface. Density Functional Theory (DFT) is used to compute adsorption energies, trace relevant orbital interactions, and discuss the electronic consequences of incorporating H to the surface. In the next sections, we will consider the computational method and adsorption models used.

2.1. Computational Method. We performed first-principles calculations based on spin-polarized DFT. The Vienna Ab initio Simulation Package (VASP) is used to solve Kohn−Sham equations with periodic boundary conditions and a plane wave basis set.[18−20] Electron−ion interactions were described by ultrasoft pseudopotentials;[21] exchange and correlation energies were also calculated using the Perdew−Burke−Ernzerhof form of the spin-polarized generalized

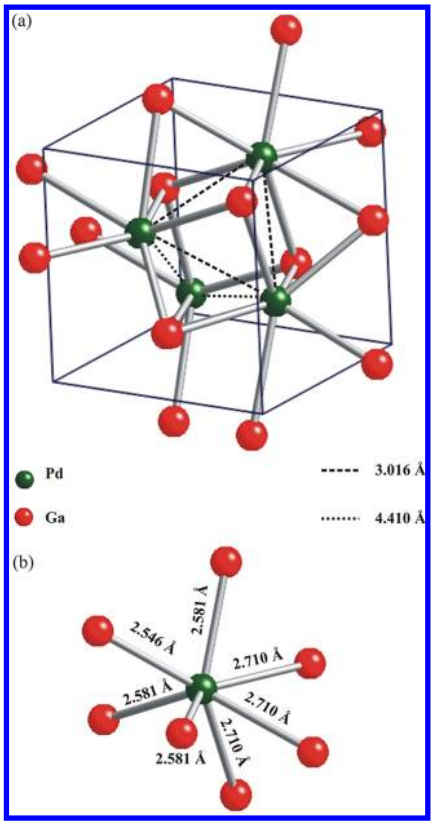

Figure 1. Unit cell of PdGa $P2_13$ (a) and bond lengths around Pd (b).

gradient approximation (GGA-PBE).[22] We used a kinetic energy cutoff of 290 eV for all calculations, which converges total energy to ∼1 meV/atom and 0.001 Å for the primitive bulk cell. The Monkhorst−Pack scheme is used for k-point sampling.[23] An equilibrium lattice constant of 4.899 Å is used, as obtained with a 7 × 7 × 7 converged mesh. This lattice constant is in agreement with experimental XRD data. Bader analysis is used to calculate electronic charges on atoms before and after H adsorption.[24] We defined the binding energy $PdGaH_n$ with respect to isolated atoms by:

$$\Delta E_{coh}(PdGa{+}nH) = E_{Total}(PdGa{+}nH) - E_{Total}(PdGa) - nE_{Total}(H_{atom}) \quad (1)$$

where n is the number of H atoms in the system.

The stabilization of $PdGaH_n$ can be better investigated by comparing the adsorption energies of $PdGaH_n$—starting from the intermetallic surface and molecular hydrogen—given by:

$$\Delta E_{ads} = E_{Total}(PdGa{+}nH) - E_{Total}(PdGa) - \frac{n}{2}E_{Total}(H_2\ \text{molecule}) \quad (2)$$

Here the first term on the right-hand side is the total energy of the super cell that includes 32 Pd and 32 Ga atoms and one or two hydrogen atoms; the second term is the total energy of the intermetallic super cell; the third term is the H atom or the half hydrogen molecule total energy; and the last one is calculated by placing H_2 in a cubic box with 10 Å sides and carrying out a Γ-point calculation. We obtained a H_2 bond length of 0.751 Å and a binding energy of −4.52 eV in fairly good agreement with experimental values.[25]

dx.doi.org/10.1021/jp302588n | J. Phys. Chem. C 2012, 116, 17518−17524

In order to understand H−PdGa interactions and bonding we used the concept of Density of States (DOS) and the Crystal Orbital Overlap Population (COOP) as described by Hoffmann.[26] The COOP curve is a plot of the OP-weighted DOS vs energy. Looking at the COOP, we analyzed the extent to which specific states contribute to a bond between atoms or orbitals.[27] The SIESTA code was used to compute COOPs.[28,29]

2.2. Surfaces and Adsorption Model. We represented the (110) plane with a super cell. In order to achieve the best compromise between computational time and accuracy of our model, we decided to use a seven-layer slab separated in the [110] direction by vacuum regions. The thickness of the vacuum region, corresponding to 10 Å, was enough to avoid the interaction of hydrogen atoms on the surfaces. The thickness of the PdGa(110) slab should be such that it approximates the electronic structure of three dimensional (3D) bulk PdGa in the innermost layer. The interlayer spacing in this PdGa(110) model is 1.745 Å. This value is not the common interplanar distance of a simple cubic structure, because every plane has atoms up, in, and above the middle line. This means that each line has three different values in the [110] direction. For the sake of clarity, Figure 2 only shows the first four layers of the slab. The (110) plane presents two possible terminated surfaces, Pd or Ga, but we analyzed only the former because it has better catalytic properties and Ga does not adsorb hydrogen.

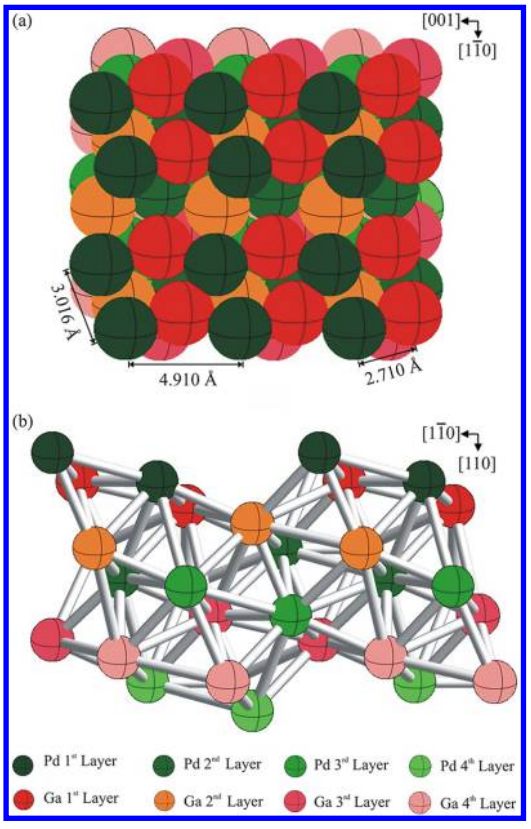

Figure 2. Pd and Ga four surface layers for the (110) surface slab. Top view (a) and side view (b).

For the study of H adsorption on the PdGa(110) surface at low coverage, the H surface distance was optimized by considering relaxation for the first four layers of the metal slab until 1 meV convergence was obtained in the total energy, maintaining the three remaining layers fixed (bulklike). H is adsorbed at a Pd top site. After optimization, a second H atom locates in the next Pd top site (see Figure 3). The adsorption energy was computed using eq 2. As mentioned in the literature, there is another mode for two-hydrogen adsorption on a single Pd atom, forming a Pd−H−H triangle.[30,31] This mode was also computed and compared for cleavage absorption of two hydrogen atoms on the two neighboring Pd atoms.

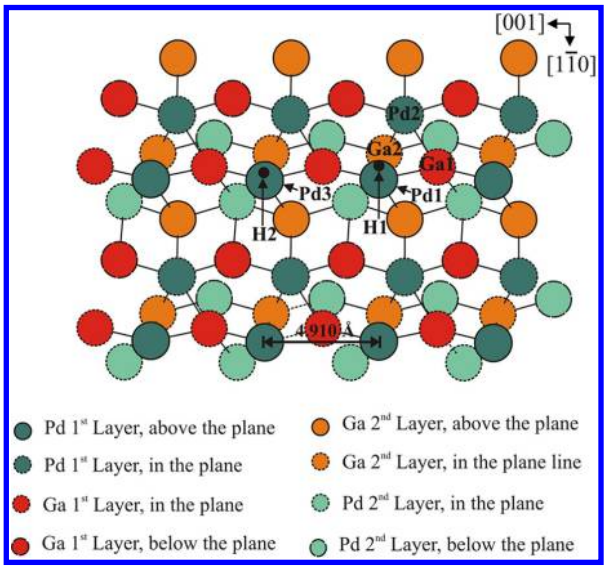

Figure 3. Schematic view of PdGa(110) surface after H adsorption. Locations on Pd and Ga on different subplanes are also shown.

3. RESULTS AND DISCUSSION

3.1. Bulk PdGa and Clean PdGa(110). The calculated value of equilibrium lattice constants a and bulk modulus B_0 slightly underestimates the experimental value results by 1% and 2%, respectively. Considering the surface of the slab, the interlayer spacing in our model changes less than 1.2% from the first to the fourth layers. The distance between two adjacent Pd top sites on the surface is 4.910 Å, and the mean Pd−Ga distance is 2.710 Å (see Figure 3).

The electronic structure for the bulk solid presents a superposition of Pd and Ga states on the whole range (see Figure 4a). Ga is represented by s- and p-like states (see s and p population in Table 1 and Figure 4c), while Pd also presents a d band with a 4.2 eV width (see Figure 4b). Our computed total DOS completely agrees with that of Kovnir et al.[3,7] In the case

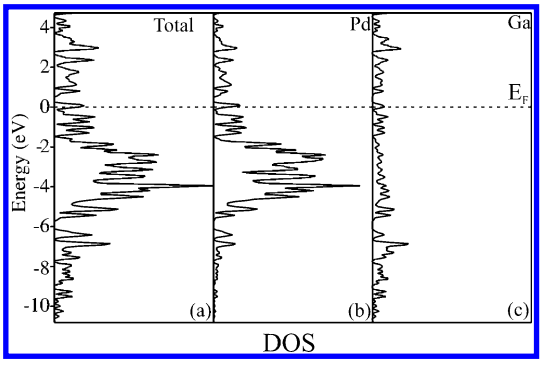

Figure 4. Total DOS curves for PdGa $P3_12$ 3D bulk (a); projected DOS for a Pd atom (b); projected DOS for a Ga atom (c).

dx.doi.org/10.1021/jp302588n | J. Phys. Chem. C 2012, 116, 17518−17524

Table 1. Electron Orbital Occupation, Overlap Population (OP), ΔOP%, and Distances for PdGa and PdGa+nH

	electron occupation						
structure	s	p	d	bond type	OP	ΔOP%	distances (Å)
Pd FCC							
Pd	0.45	0.27	9.27	Pd−Pd	0.102		2.750
PdGa bulk							
Pd	0.72	0.45	9.68	Pd−Pd	0.090		3.012
Ga	1.69	0.46	0.00	Pd−Ga	0.132		2.710
PdGa slab							
Pd 4th layer	0.71	0.42	9.70	Pd−Pd	0.086		3.016
Ga 4th layer	1.68	0.45	0.00	Pd−Ga	0.130		2.709
PdGa(110)							
Pd	0.80	0.22	9.88	Pd1−Pd2	0.142		3.016
Ga	1.71	0.44	0.00	Pd1−Ga1	0.137		2.710
PdGa + 1H							
Pd	0.61	0.58	9.76	Pd1−Pd2	0.064	−54.9	3.023
Ga	1.74	0.35	0.00	Pd1−Ga1	0.126	−8.0	2.592
H	1.32	0.00	0.00	Pd1−H1	0.643		1.621
PdGa + 2H							
Pd	0.60	0.57	9.75	Pd1−Pd2	0.053	−62.7	3.012
Ga	1.75	0.30	0.00	Pd1−Ga1	0.137	–	2.569
H	1.33	0.00	0.00	Pd1−H1	0.640		1.619
				Pd3−H2	0.642		1.620

of the surface, the d bandwidth decreases 0.2 eV with regard to bulk states.

As reported before, the PdGa compound presents a significantly reduced electron density at the Fermi level (see Figure 4a) and shifts the Pd 4d band to higher binding energies compared to pure FCC Pd.[7] The PdGa(110) surface shows this behavior in the decomposed (s-p-d) states near E_F (see Figure 5a−c). The valence band synchrotron XPS spectrum of cleaned

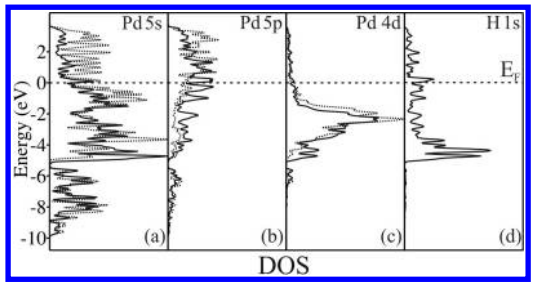

Figure 5. Orbital decomposition for projected DOS curves for Pd1 before and after one H adsorption (a−c) (dotted and full line, respectively). Projected DOS curves for H1 after adsorption (d).

Pd and PdGa detects a strong decrease in bands intensity near E_F for the intermetallic compound.[7] Recent specific heat measurements have shown that the DOS of PdGa at the Fermi level is reduced to 15% of the DOS of FCC Pd.[9] Rosenthal et al. also measured depleted states in the photoemission spectrum for PdGa near E_f.[14]

A substantial number of p states penetrate the d band. Dispersion of the s and p bands is much larger than that of the d band, thus showing the more contracted nature of d orbitals. If we look at the detailed composition of, say, the bulklike fourth layer of the slab, we obtain the orbital electron occupation: Pd $d^{9.70}$ $s^{0.71}$ $p^{0.42}$ and Ga $s^{1.68}$ $p^{0.45}$, which is close to Pd $d^{9.68}$ $s^{0.72}$ $p^{0.45}$ and Ga $s^{1.69}$ $p^{0.46}$, obtained for the bulk PdGa. According to previous calculations[3] and elements electronegativity[32] Pd is negatively charged. Our results in Table 1 show the total electron occupation for Pd (in PdGa) $10.85e^-$ in contrast to elementary FCC Pd ($9.99e^-$). A higher degree of filling for the d-band—compared to elemental Pd—is also computed in the surface: 9.88 for Pd in PdGa(110) vs 9.27 in the FCC Pd. The last result is in agreement with those reported in the literature.[7]

For the Pd-terminated surface, the calculated orbital electron occupation is Pd $d^{9.88}$ $s^{0.80}$ $p^{0.22}$ and Ga $s^{1.71}$ $p^{0.44}$. The orbitals of the surface atoms in the surface layers have somewhat less dispersion, i.e. they form narrower bands. There are fewer nearest neighbors—4 for Pd and 5 for Ga—surface atoms compared to those for the inner atoms—7 for Pd and 6 for Ga. The decrease in coordination reduces the number of overlaps

Table 2. Orbital-by-Orbital Percentage Contributions to Pd1−Pd2, Pd1−Ga1, and Pd1−H1 Overlap Populations (%COOP) for PdGa(110) + *n*H System

	Pd1−Pd2			Pd1−Ga1			H1	
	PdGa(110)	PdGa+1H	PdGa+2H	PdGa(110)	PdGa+1H	PdGa+2H	PdGa+1H	PdGa+2H
s−s	40.6	12.9	8.5	13.3	10.9	9.8	51.4	51.3
s−p	35.7	41.1	37.0	67.4	57.1	57.3	46.7	46.4
s−d	5.4	6.8	12.5	0	0	0	1.9	2.1
p−p	5.5	11.4	7.9	11.8	12.5	11.9	–	–
p−d	12.2	27.8	34.1	7.5	19.5	21.0	–	–
d−d	0.0	0.00	0.0	–	–	–	–	–

dx.doi.org/10.1021/jp302588n | J. Phys. Chem. C 2012, 116, 17518−17524

available to the atom, and this eventually controls the bandwidth. The DOS decomposition in Figure 4a in bulk (dotted line) and surface shows this effect. The surface atom states are less dispersed and few of them go above E_F.

Regarding the bonding, OP for Pd−Pd and PdGa 3D bulk are 0.090 and 0.132, while in the surface they are 0.142 and 0.137, respectively (see Table 1). In the slab, the Pd−Pd and Pd−Ga bulklike atoms present an OP of 0.086 and 0.130, which are very close to the value in the 3D alloy.

Orbital-by-orbital contributions to the OP between atoms in the PdGa surface are summarized in Table 2. The main interactions are s−s and s−p followed by d−p and d−s. No d−d interaction is detected. Recent NMR results indirectly confirm the covalent bonding scheme between Ga and Pd atoms.[9]

3.1. Hydrogen Adsorption on the Relaxed PdGa(110): Low Coverage. We found one H bond on the top Pd site (see Figure 3) at a Pd−H distance of 1.621 Å and stabilization energy of −0.70 eV (eq 1). The Pd−H bond length is close to the sum of the atomic radii of Pd and H, and no Ga−H interaction is detected. The on-top site is predicted to be endothermic with respect to gaseous H_2 and a clean PdGa surface by +0.44 eV—as defined in eq 2. Our prediction of the site geometry can be compared to calculations on metallic FCC Pd(100) surface; where the Pd−Pd nearest neighbor distance is 2.76 Å. Tománek et al.[33] reported a stabilization energy of −1.86 eV and a bond length of 1.56 Å for H on top on Pd(100). Dong and Hafner predicted H_2 dissociation on top−top sites to be unstable on FCC Pd(111) at a H−Pd distance of 1.55 Å.[34] Our theoretical predictions are in agreement with the experimental results obtained by Klanjšek[9] that detect no hydrogen adsorption as required for good hydrogenation catalysis. Clearly, hydrogen will only adsorb dissociatively if the net energy gain is $\Delta E_{Hads} > 0$. This is not the case for one hydrogen atom. However, the situation is reverted to −0.55 eV if two hydrogen atoms are considered simultaneously on top of two adjacent Pd sites: −0.275 eV/H atom and Pd−Pd is 4.910 Å. If we refer the adsorption of two hydrogen atoms to two isolated H atoms, the stabilization energy is −2.85 eV (−1.425 eV/H atom). It should be pointed out that, due to geometric constraints in the case of H/PdGa(110), the natural adsorption site is a Pd top. A similar result for the top site is reported in a recent review of adsorption and absorption in the hydrogen−palladium system published by Jewell and Davis.[35] The largest distance among Pd atoms is 4.910 Å (Pd1−Pd3 in Figure 3) and the shortest distance (Pd1−Pd2) is 3.016 Å; compared to elemental Pd (2.750 Å) this could be one of the reasons for the higher selectivity of PdGa as a hydrogenation catalyst.[9]

The subsurface hydrogen on transition metals and near-surface alloys is typically endothermic with respect to gas-phase H_2(g).[36] The role of subsurface hydrogen on the adsorption of ethylene on Pd(111) and Pd nanoparticles was previously described[37,38] The covalence of Pd−Ga bonding prevents the formation of subsurface hydrides and reduces hydrogen supply for unselective hydrogenation and, thus, enhances selectivity. This was confirmed by Prompt Gamma Activation Analysis (PGAA).[7] Our computed energy for a subsuperficial H on PdGa(110) surface is completely unstable, and this is in agreement with previous experimental findings.[7] In the case of adsorption of two hydrogen atoms on the same Pd site, our results indicate a favorable geometry as predicted before for Pd/graphene.[30] However, this structure is 0.40 eV less stable than the adsorption on two isolated Pd sites, each of them with one hydrogen atom. This adsorption geometry could be present at higher hydrogen coverages.

Considering the electronic structure, we found no significant change in the Fermi level after H adsorption, as expected. The total DOS is dominated by the many bulklike and surface Pd and Ga atoms, so that the changes are subtle. On bonding to the surface, electron transfer occurs from Pd atoms to H atoms to the extent of 0.33 e^-. The structure of PdGa was studied using several methods such as CO-adsorption, in situ XPS, and PGAA.[7] XPS results show that there is no change in the electronic structure of the surface upon reaction conditions. This conclusion is in full agreement with our results on the effect of hydrogen on the electronic structure of the PdGa(110) surface.

Figure 6a shows the total DOS of the system with H contribution. The bar on the right in the DOS plots indicates

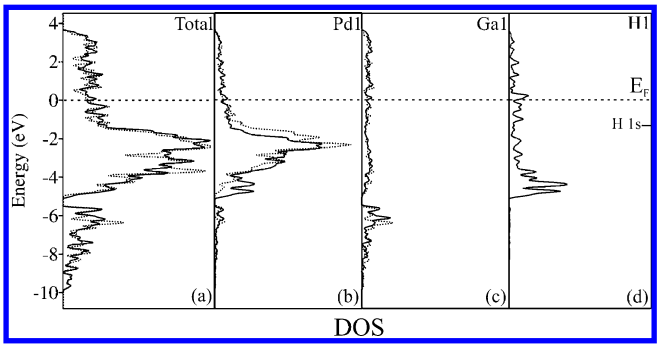

Figure 6. Total DOS curves for 2H/PdGa(110) (a); projected DOS for a Pd atom (b); projected DOS for a Ga atom (c); and projected DOS for a H atom (d). Before and after one H adsorption (dotted and full line, respectively). The bar on the right indicates the energy level of H 1s relative to E_F before adsorption.

the energy level of the H 1s orbital before interaction. We did not find a split-off H−Pd state below the bottom of the d band (see Figure 6d at −5 eV). Similar results were reported by Tománek et al.[33] in the case of H adsorption on top on Pd(100). These split-off states are clearly present in Pd hydrides.[39] The presence of the stabilizing H split-off states in the DOS was detected in the study of H-induced reconstruction on Pd(110). H is adsorbed on a four-fold site at a Pd−H distance of 2.11 Å.[40]

An analysis of the bonding between H and the surface reveals that the main contribution to the Pd−H bond comes from H 1s and Pd 5s and $5p_z$ orbitals and less than 3% from the remaining orbitals (see Table 2). The states between (−6, −4) eV (Figure 6d) are composed of 51% s, 47% p, and about 2% d states.

As can be seen in Table 1, the H−Pd bonding is achieved at the expense of weakening Pd1−Pd2-nearest neighbor in Figure 3 at 3.016 Å. Thus, the Pd1−Pd2 bond OPs involving Pd atoms directly bonded to H is reduced to 55% of its original value on the clean PdGa surface. Comparing COOP curves for the Pd bonded to H with Pd1−Pd2 in the clean surface (Figure 7a), it can be seem that bonding states at 1.1 eV are not present after H adsorption, thus making the Pd1−Pd2 interaction less bonding. The Pd−Ga OP presents small changes (see Figure 7b), and this is mentioned before any Ga−H bonding interaction is detected. The bond length is 5% shorter after H adsorption. When a second H is considered on the nearest neighbor Pd top site, only an additional 7% drop in Pd1−Pd2 OP is detected. In conclusion both H1−Pd1 and H2−Pd3

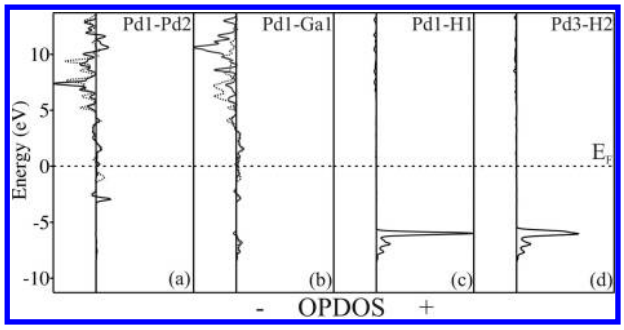

Figure 7. Pd−Pd, Pd−Ga, and Pd−H COOP curves for PdGa(110) surface with one (a−c) and two hydrogens (d).

behave as "isolated sites" where Ga plays the role of diluent and the alloy maintains the structural array of site isolation. These results are in agreement with the concept of "site isolation" experimentally explored by Kovnir et al.[7]

Finally, we also computed the vibration frequency of H bonded to the surface. In order to do this, we used a whole vibrational mode with important contributions for the Pd−H bond. The computed vibration frequency for this bond is 1669.82 cm^{-1}, and for the Pd-slab it is 112.13 cm^{-1}. This result shows some analogy with that reported by Tománek et al. in the case of H/Pd(100) and H/Pd(110) −1750.54 and 2121.62 cm^{-1}, respectively. More recently, Andrews et al.[41] computed the infrared spectra of Pd(H_2) complexes in solid argon. The predicted Pd−H bond length was 1.54 1 Å, and the vibration frequency was in the range of 1400−2000 cm^{-1}, depending on the functional basis or pseudopotential used. Unfortunately, no experimental data is available for H/PdGa(110) alloy surface.

It is worth mentioning some results obtained from FT-IR studies. This is the case for CO adsorption on PdGa and Pd/Al_2O_3 samples. The complete isolation of Pd on the PdGa surface shows a significant red shift of CO vibrational frequency at 2047 cm^{-1}. This band was assigned to CO adsorption on Pd in the on-top position, the red-shift being a result of negatively charged Pd.[7] Low-temperature experiments revealed a fine structure of the adsorption bands and were attributed to at least three different isolated Pd atoms. These facts will be the aim for future theoretical calculations.

4. CONCLUSION

The electronic structure of H in $P2_13$ PdGa alloy has been studied by DFT calculations. The following cases were studied: one or two hydrogen atoms at two adjacent Pd top sites on the (110) surfaces.

H adsorption is −0.70 eV stable, with respect to the isolated atom, but it is 0.44 eV unstable with respect to the gaseous H_2 molecule. However, when two hydrogen atoms are considered, the adsorption energy is −1.425 eV/atom. These results are analogous to those computed on top sites on FCC (100) or (110) Pd metallic surfaces.

Pd−H interaction occurs mainly via Pd 5s−H1s and 5p−H1s orbitals with a small contribution of 4d orbitals. H is found negatively charged. The Pd−H bond is formed at the expense of Pd−Pd bonding. Our results are in agreement with related calculations on Pd FCC surfaces[33,34] and PdGa alloys.[3,7] No Ga−H interaction is detected, and the second hydrogen interacts with the neighboring Pd top site in an "isolated way" as revealed by both DOS and COOP curves.

The Pd−H bond length vibration frequency is close to that of similar bonds in both open metallic surfaces and diatomic molecules in solid argon.[33,41]

AUTHOR INFORMATION

Corresponding Author

*E-mail: cajuan@uns.edu.ar. Telephone: +54-291-4595101, ext. 2818. Fax: 54-0291-4595142.

Notes

The authors declare no competing financial interest.

ACKNOWLEDGMENTS

Our work was supported by ANPCyT through PICT 1770, and PIP-CONICET No.114-200901-00272 and No.114-200901-00068 Research Grants, as well as by SGCyT-UNS. A.J., E.G., and P.J. are members of CONICET. P.B. is a fellow researcher at this institution. We kindly acknowledge the important suggestions made by our reviewers and the useful discussions with Prof. E. Pronsato.

REFERENCES

(1) Bos, A. N. R.; Westerterp, K. R. *Chem. Eng. Process* **1993**, *32* (1), 1−7.
(2) Figueras, F.; Coq, B. *J. Mol. Catal. A: Chem.* **2001**, *173* (1−2), 223−230.
(3) Kovnir, K.; Armbrüster, M.; Teschner, D.; Venkov, T. V.; Jentoft, F. C.; Knop-Gericke, A.; Grin, Y.; Schlogl, R. *Sci. Technol. Adv. Mater* **2007**, *8* (5), 420−427.
(4) Molnar, A.; Sarkany, A. *J. Mol. Catal. A: Chem.* **2001**, *173* (1−2), 185−221.
(5) Osswald, J.; Giedigkeit, R.; Jentoft, R. E.; Armbruster, M.; Girgsdies, F.; Kovnir, K.; Ressler, T.; Grin, Y.; Schlogl, R. *J. Catal.* **2008**, *258* (1), 210−218.
(6) Osswald, J.; Kovnir, K.; Armbrüster, M.; Giedigkeit, R. *J. Catal.* **2008**, *258*, 219−227.
(7) Kovnir, K.; Armbrüster, M.; Teschner, D.; Venkov, T. V.; Szentmiklosi, L.; Jentoft, F. C.; Knop-Gericke, A.; Grin, Y.; Schlogl, R. *Surf. Sci.* **2009**, *603* (10−12), 1784−1792.
(8) Armbrüster, M.; Kovnir, K.; Teschner, D.; Behrens, M.; Grin, Y.; Schlogl, R. *J. Am. Chem. Soc.* **2010**, *132*, 14745−14747.
(9) Klanjšek, M.; Gradišek, A.; Kocjan, A.; Bobnar, M.; Jegli, P.; Wencka, M.; Jaglicic, Z.; Popcevic, P.; Ivkov, J.; Smontara, A.; Gille, P.; Armbrüster, M.; Grin, Y.; Dolinšek, J. *J. Phys.: Condens. Matter* **2012**, *24*, 085703 (9pp).
(10) Armbrüster, M.; Kovnir, K.; Grin, Y.; Schlögl, R. In *Complex Metallic Alloys: Fundamentals and Applications*; Dubois, J. M., Belin-Ferré, E., Eds.; Wiley-VCH: Weinheim, 2011; pp 385−399.
(11) Armbrüster, M.; Wowsnick, G.; Friedrich, M.; Heggen, M.; Cardoso-Gil, R. *J. Am. Chem. Soc.* **2011**, *133*, 9112−9118.
(12) Ota, A.; Armbrüster, M.; Behrens, M.; Rosenthal, D.; Friedrich, M.; Kasatkin, I.; Girgsdies, F.; Zhang, W.; Wagner, R.; Schlogl, R. *J. Phys. Chem. C* **2011**, *115*, 1368−1374.
(13) Shao, L.; Zhang, W.; Armbrüster, M.; Teschner, D.; Girgsdies, F.; Zhang, B.; Timpe, O.; Friedrich, M.; Schlogl, R.; Su, D. S. *Angew. Chem., Int. Ed.* **2011**, *50*, 10231−10235.
(14) Rosenthal, D.; Widmer, R.; Wagner, R.; Gille, P.; Armbrüster, M.; Grin, Y.; Schlogl, R.; Gröninh, O. *Langmuir* **2012**, *28*, 6848−6856.
(15) Hellner, E.; Laves, F. *Z. Naturforsch* **1947**, *A2*, 177−183.
(16) Bhargava, M. K.; Gadalla, A. A.; Schubert, K *J. Less-Common Met.* **1975**, *42*, 69−76.
(17) Phragmen, G. *Jernkontor. Ann.* **1923**, *107*, 121.
(18) Armbrüster, M.; Borrmann, H.; Wedel, M.; Prots, Y.; Giedigkeit, R.; Gille, P. *Z. Kristallogr.-New Cryst. Struct.* **2010**, *225*, 617−618.
(19) Kresse, G.; Hafner, J. *Phys. Rev. B* **1993**, *47*, 558−561.
(20) Kresse, G.; Furthmüller, J. *Phys. Rev. B* **1996**, *54*, 11169−11186.
(21) Kresse, G.; Furthmüller, J. *Comput. Mater. Sci.* **1996**, *6*, 15−50.

(22) Vanderbilt, D. *Phys. Rev. B* **1990**, *41*, 7892−7895.
(23) Perdew, J.; Chevary, J. A.; Vosko, S. H.; Jackson, K. A.; Pederson, M. R.; Singh, D. J.; Fiolhais, C. *Phys. Rev. B* **1992**, *46*, 6671−6687.
(24) Monkhorst, H. J.; Pack, J. D. *Phys. Rev. B* **1976**, *13*, 5188−5192.
(25) Bader, R. F. W. *Atoms in Molecules: A Quantum Theory*; Oxford University Press: Oxford, 1990.
(26) Huber, K. P.; Hertzberg, G. *Molecular Spectra and Molecular Structure IV: Constants of Diatomic Molecules*; Van Norstrand Reinhold: New York, 1979.
(27) Hoffmann, R. *Solid & Surface: A Chemist's View of Bonding in Extended Structures*, 1st ed.; VCH: New York, 1989.
(28) Ordejón, P.; Artacho, E.; Soler, J. M. *Phys. Rev. B* **1996**, *53*, R10441−R10444.
(29) Soler, J. M.; Artacho, E.; Gale, J. D.; Garcia, A.; Junquera, J.; Ordejón, P.; Sanchez-Portal, D. *J. Phys. Condens. Matter* **2002**, *14*, 2745−79.
(30) López-Corral, I.; Germán, E.; Juan, A.; Volpe, M. A.; Brizuela, G. P. *J. Phys. Chem. C* **2011**, *115* (10), 4315−4323.
(31) López-Corral, I.; Germán, E.; Juan, A.; Volpe, M. A.; Brizuela, G. P. *Int. J. Hydrogen Energy* **2012**, *37*, 6653−6665.
(32) Sanderson, R. T. *Chemical Bonds and Bond Energy*; Academic Press: New York, 1976.
(33) Tománek, D.; Sun, Z.; Louie, S. G. *Phys. Rev. B* **1991**, *43*, 4699−4713.
(34) Dong, W.; Haffner, J. *Phys. Rev. B* **1997**, *56*, 15396−15403.
(35) Jewell, L.; Davis, B. H. *Appl. Catal., A* **2006**, *310*, 1−15.
(36) Greeley, J.; Mavrikakis, M. *J. Phys. Chem. B* **2005**, *109*, 3460−3471.
(37) Stacchiola, D.; Tysoe, W. T. *Surf. Sci.* **2003**, *540*, L600−L604.
(38) Ludwig, W.; Savara, A.; Madix, R. J.; Schauermann, S.; Freund, H.-J. *J. Phys. Chem. C* **2012**, *116*, 3539−3544.
(39) Chan, C. T.; Louie, S. G. *Phys. Rev. B* **1983**, *27*, 3325−3337 and references therein..
(40) Ledentu, V.; Dong, W.; Sautet, P.; Kresse, G.; Hafner, J. *Phys. Rev. B* **1998**, *57*, 12482−12491.
(41) Andrews, L.; Wang, X.; Alikhani, M. E.; Manceron, L. *J. Phys. Chem. A* **2001**, *105*, 3052−3063.